Inter-Research Science Publisher

Endangered Species Research
Volume 56:323–337

Published April 24, 2025
https://doi.org/10.3354/esr01397

Tracking trends in foraging sea turtle aggregations at Reunion Island using aerial and photo-ID surveys (2008–2023)

Antoine Laforge[1,*], Katia Ballorain[1], Anne-Emmanuelle Landes[1], Jérôme Bourjea[2], Stéphane Ciccione[3], Claire Jean[3]

[1]Centre d'Étude et de Découverte des Tortues Marines (CEDTM), 19 rue des Frangipaniers, 97424 Saint Leu, La Réunion, France
[2]MARBEC, Université de Montpellier, CNRS, IFREMER, IRD, 34200 Sète, France
[3]Kelonia, l'observatoire des tortues marines, 46 rue du Général de Gaulle, 97436 Saint Leu, La Réunion, France

ABSTRACT: The sea turtle populations of Reunion Island, a volcanic island in the western Indian Ocean between Madagascar and Mauritius, were significantly impacted by human colonization in the 17th century. However, after 40 yr of local and regional conservation efforts, these populations are showing signs of recovery. This study examines spatiotemporal trends in the abundance and distribution of green turtles *Chelonia mydas* and hawksbill turtles *Eretmochelys imbricata* along the west coast of Reunion Island from 2008 to 2023. Data were collected through microlight aerial surveys and photo-ID. The results reveal a consistent increase in turtle abundance, particularly juveniles, with juvenile green turtles comprising 78%, juvenile hawksbill turtles 15%, and the remaining observations based on photo-ID being adult green turtles. Size-class estimates from aerial surveys suggest that annual fluctuations in abundance are derived largely from variations in the number of smaller turtles, underscoring Reunion Island's role as a critical developmental habitat. The highest concentrations of turtles were observed in fringing reef areas characterized by shallow, gently sloping bathymetric zones. Photo-ID also revealed strong site fidelity for both species. Combining aerial surveys and photo-ID — an innovative approach — this study provides life-stage-specific abundance trends across 9% (5.5 km^2) of the surveyed area (60 km^2) and links distribution patterns to food availability. Notably, in one area, a decline in green turtles correlates with the loss of seagrass habitat. These findings advance understanding of the spatial ecology of in-water turtles and offer valuable insights for local and regional conservation planning. They further emphasize the role of sea turtles as indicators of coastal ecosystem health.

KEY WORDS: *Eretmochelys imbricata* · *Chelonia mydas* · Coastal distribution · Aerial survey · Photo-identification · Reunion Island

1. INTRODUCTION

After years of oceanic development, juvenile green turtles *Chelonia mydas* and hawksbill turtles *Eretmochelys imbricata* recruit to neritic habitats to which they exhibit high fidelity (Schofield et al. 2010, Chambault et al. 2020, Siegwalt et al. 2020, Sanchez et al. 2024), and later on as adults between reproductive cycles (Shimada et al. 2020). However, the increasing human activities in coastal regions are placing significant pressure on sea turtle populations (Hamann et al. 2010, Lutcavage et al. 1997) and their coastal habitats worldwide (Halpern et al. 2008). Because sea turtles play multiple roles in these coastal ecosystems, their presence is a good indicator of the overall health of the habitat they use (Aguirre et al. 2002). Therefore, monitoring sea turtle abundance may allow for indirect monitoring of the global health of the habitats, in addition to the human-induced pressures and the potential impacts on these threatened species (Aguirre & Lutz 2004, Komoroske et al. 2011). Despite an increasing number of international conservation

*Corresponding author: antoine.laforge8@gmail.com

Publisher: Inter-Research · www.int-res.com

agreements strengthening the legal protection framework, hawksbill turtles are listed by the International Union for Conservation of Nature (IUCN) as globally Critically Endangered (Mortimer & Donnelly 2008) and green turtles globally as Endangered (Seminoff 2023), although a recent regional assessment indicated that in some regions, the regional population of green turtles is listed by the IUCN as Least Concern (e.g. western Indian Ocean; Bourjea & Dalleau 2023). The recently updated global conservation assessment further classifies the Southwest Indian Ocean Regional Management Units (RMUs) for both green and hawksbill turtles as facing low risk and low threat levels (Wallace et al. 2025).

Reunion Island, located in the southwestern Indian Ocean, was first described by early colonists in the 17th century as an important nesting site for green turtles (Deschamps 1962). However, centuries of sea turtle hunting and egg harvesting following human colonization led to a dramatic decline in both nesting and foraging sea turtle populations (Hughes 1974, Frazier 1975, Bertrand et al. 1986). After a 25 yr absence, a limited but promising return of nesting activity was observed in 2004–2005, with the documentation of 11 green turtle nests (Ciccione & Bourjea 2006). To date, no hawksbill turtle nesting activity has been observed or documented in the literature for Reunion Island. Furthermore, juvenile green and hawksbill turtles have been consistently observed foraging year-round in neritic habitats along Reunion Island's coastline (Ciccione 2001, Ballorain et al. 2010, Chassagneux et al. 2013, Chambault et al. 2020). Aerial surveys conducted between 1998 and 2008 indicated an increase in in-water sea turtle aggregations off the west coast (Jean et al. 2010a). The establishment of the Kelonia Sea Turtle Observatory in 2006, which focuses on rehabilitating injured turtles while raising public awareness, has created a supportive framework for protecting the local sea turtle population. In 2007, the creation of the Reunion Natural Marine Reserve, covering 35 km^2 of coastline in the northwest of the island, has reinforced the initiative to protect marine habitats, home to important biodiversity, including sea turtles. At the same time, Reunion Island's growing human population (+0.5% yr^{-1} from 2009 to 2020, estimated at 871 200 in 2021; INSEE 2025) continues to increase the pressure on its coastal marine habitats. Urban development, tourism, and maritime activities contribute to pollution and habitat degradation, posing significant threats to these environments (Philippe et al. 2016).

In this context, the recent shifts in the distribution and dynamics of the local sea turtle population at Reunion Island remain poorly understood. Having an overview of the spatiotemporal distribution, along with life stage and species proportions, is key to being able to evaluate and guide conservation measures. Furthermore, due to the strong regional connectivity between nesting and foraging habitats in the western Indian Ocean (Bourjea & Dalleau 2015, Nivière et al. 2024), local data on population status is essential to assess population trends at a regional scale.

Since 1998, aerial surveys have been conducted to count sea turtles surfacing along reef drop-offs or rocky shores from Pointe au Sel to Le Port (see Fig. 1) (Sauvignet et al. 2000). In September 2012, the transect was extended southward to begin at St. Pierre, ensuring coverage of the marine reserve and additional reefs outside its boundaries. Aerial surveys are widely recognized as the most effective method for monitoring wildlife over large areas (Caughley 1977). They have been extensively applied in sea turtle research (Roos et al. 2005, Fuentes et al. 2006, Lauriano et al. 2014, Benson et al. 2020, Pierantonio et al. 2023), which has facilitated the measurement of spatiotemporal population trends. However, these surveys are limited in their ability to provide detailed information on population structure, such as life stages, hardshell species differentiation, or individual movements. To address these gaps, a photo-identification (photo-ID) programme — Photo-identification of Sea Turtles on Reunion Island — was launched in 2007 (Jean et al. 2010b). The method is based on the temporal stability of the scale patterns on both sides of the head (Reisser et al. 2008, Schofield et al. 2008). By complementing aerial surveys, this method partially bridges the data gap, enabling finer-scale analyses of aggregation structure (Jean et al. 2010b, Chassagneux et al. 2013, Dunbar et al. 2021).

In this study, we use both methods separately and in combination to (1) analyse spatiotemporal trends in sea turtle abundance, (2) examine species and life stage trends in areas where the 2 methods overlap, and (3) track individual turtle movements relative to their most frequently observed locations. This unique approach aims to provide a comprehensive perspective on sea turtle population structure, distribution, and trends, providing critical insights for developing targeted conservation strategies at the local scale.

2. MATERIALS AND METHODS

Data from aerial surveys and photo-ID were collected along the west coast of Reunion Island (21° 6′ S, 55° 30′ E). The 62 km of coastline between St. Pierre

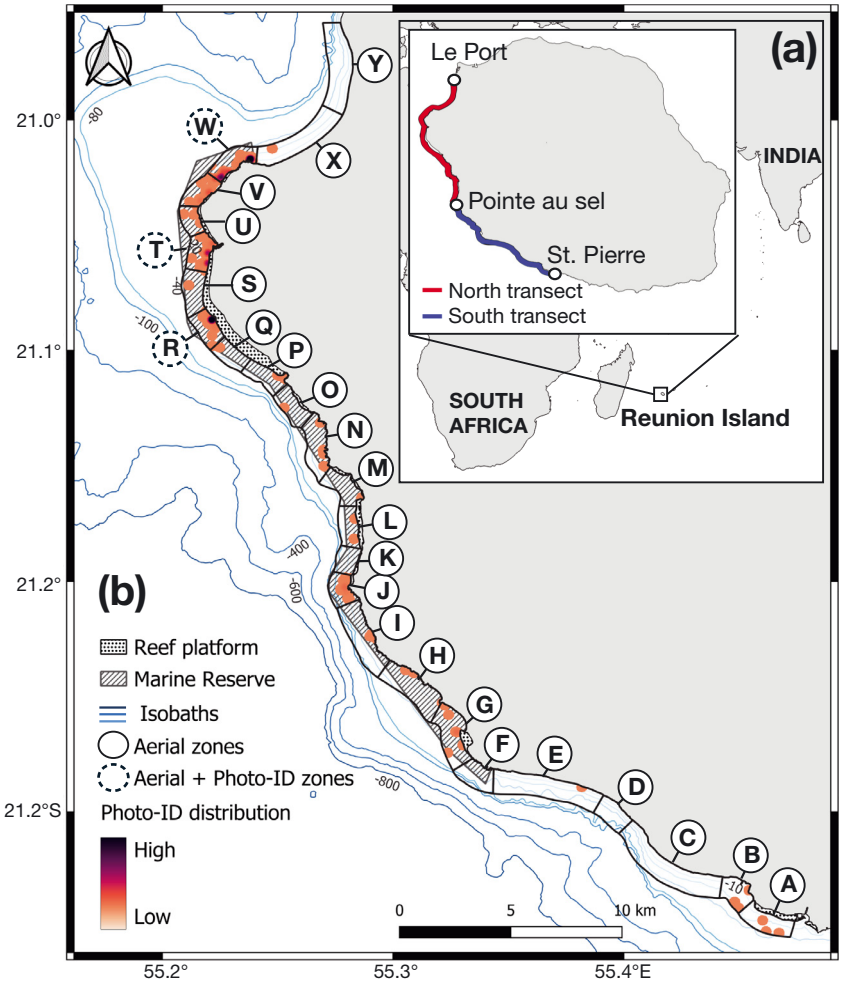

Fig. 1. Aerial survey area along the west coast of Reunion Island, extending from St. Pierre to Le Port. (a) Reunion Island in the western Indian Ocean, highlighting the south and north aerial transects. (b) Detailed subdivision of the aerial strip into 25 zones (A–Y), including marine reserve boundaries, isobath contours (10, 20, 40, 80, 100, 400, 600, 800 m), reef platforms, and the distribution of photo-ID data based on current knowledge of home ranges in the region. Zones W, T, and R are identified as areas where photo-ID distribution covers ≥50% of the zone and where ≥10 sightings have been recorded over a 2 yr period

and Le Port (Fig. 1a) is protected from trade winds and major weather events by important relief features and includes all of the island's reef platforms, most of its coral reefs, and major seagrass beds (Turner & Klaus 2005, Cuvillier et al. 2017)

2.1. Field methods

2.1.1. Aerial surveys

The CEDTM-Kelonia initiated aerial surveys in July 1998, initially targeting the coastline from Pointe au Sel to Le Port (Sauvignet et al. 2000), hereinafter referred to as the north region (highlighted in red on Fig. 1a). However, due to significant changes in the aerial survey protocol in 2008 to standardize the data collection process, data collected prior to 2008 are not included in the study. In September 2012, the standardized transect was extended further south to begin at St. Pierre, increasing the length of coastline surveyed from 34 to 62 km (south region; in blue on Fig. 1a).

The transect consisted of following sinusoids (average wavelength = 1.2 km) between the coastline or reef barrier and approximately 1.5 km offshore. Observations were recorded from aboard a tandem-seat microlight aircraft (Rans S-7 Courier) with a high wing configuration that allows for a side viewing platform and the transport of 2 people (the pilot and 1 observer). Transects were flown at an average elevation of 200 m (SD = 40 m) and at an average speed of 90 km h^{-1}. The frequency of flights (on average every 1–2 mo) depended on the availability of the pilot, the aircraft, and the occurrence of standard meteorological conditions (<7 knots [13 km h^{-1}] wind, <2 m swell, and <20% cloud cover). An observer marked the GPS position (handheld GPS Garmin) of (sub-)surfacing turtles located directly below or near the aircraft. New observers, after ground training, were paired with experienced pilots who ensured an optimal flight path and assisted in initial turtle spotting, to minimize the effect of inexperience.

Covariates collected during the survey included a rough visual estimate of size class (small: size < 0.5 m; medium: 0.5 m < size < 1 m; large: size > 1 m; and NA when size assessment was not possible), launch time, and meteorological conditions (optimal, suitable, average). The exact trajectory of the transects was recorded by GPS (1 location s^{-1}).

2.1.2. Photo-ID

CEDTM-Kelonia initiated the photo-ID programme — Photo-identification of Sea Turtles on Reunion Island — on Reunion Island in 2007 (https://museesreunion.

fr/kelonia/actualites-et-savoirs-de-kelonia/la-photo-identification-des-tortues-marines/). This programme identifies individuals by analysing the unique arrangement of head scales, following the procedure described in Jean et al. (2010b) and Dunbar et al. (2021). Data are collected opportunistically mainly in highly used dive spots by SCUBA divers participating in a citizen science programme. As a result, sampling effort varies across years and sites. The data submitter provides photos or videos, site name (dive buoy/site location or GPS position), and date. An experienced user then converts each head profile into a code in the TORSOOI platform (www.torsooi.org) along with information on species, life stage, and sex (Jean et al. 2010b).

Identifying a new individual requires profiles of both sides of the head. Profiles lacking a corresponding match are stored as partial identifications until another opportunistic encounter captures both head profiles, enabling complete identification. Once completed, the previously unlinked profiles are integrated with the turtle's identification history in the database.

2.2. Data analysis

2.2.1. Correspondence between aerial and photo-ID datasets

To align the timeframes of the standardized aerial surveys (2008–present) and the photo-ID programme (2007–present), this study focused on a 16 yr dataset spanning 2008 to 2023. A 2 yr window (hereinafter referred to as 'year$_2$') was arbitrarily chosen to pool the data as the best compromise between temporal resolution and sufficient sampling for robust statistical analysis.

To combine aerial and photo-ID data, we tried to define areas where both sampling efforts overlapped sufficiently. To achieve this goal, the first step is to estimate the distribution of aerial survey effort and the distribution of photo-ID data on the same grid (5 m pixel grid). Aerial survey effort is estimated by applying a Gaussian kernel density estimator (KDE) to all sampling points from the GPS tracks using a 250 m radius (corresponding to an estimated 50% probability of detecting a sea turtle at a similar altitude; Benson et al. 2007, Lauriano et al. 2011). The area of uniform aerial survey effort (hereinafter referred to as the aerial strip, surface = 60 km^2) is defined by a strip bounded by the shoreline and a threshold of 50 sampling points per pixel (see Fig. S1 in Supplement 1 at www.int-res.com/articles/suppl/n056p323_supp.pdf; for all supplements). To align photo-ID and aerial surveys, only photo-ID data reported within the aerial strip are retained. In order to evaluate the distribution of the photo-ID data, it is necessary to determine the radius associated with the photo-ID locations. In practice, without knowing exactly where a diver photographed a turtle, photo-ID locations correspond to a larger area represented by the diver's exploration zone. In addition, green and hawksbill turtles in neritic habitats are known to occupy a limited area commonly referred to as the home range (Makowski et al. 2006, Berube et al. 2012). Due to the difficulty in estimating the diver's exploration zone, which can vary between sites and divers' motivation and experience, we assumed that each photo-ID location can be associated with individual home ranges, which are assumed to be larger than the diver's exploration zone. Chambault et al. (2020) demonstrated that 11 tagged juvenile green turtles on the west coast of Reunion Island occupied a maximum area of 0.2 km^2 (50% kernel area). Since juvenile green turtles make up the majority of the Reunion Island population (Chassagneux et al. 2013), we chose a radius of 250 m (radius of a 0.2 km^2 circle) to calculate the photo-ID distribution using a Gaussian KDE (see red heat map in Fig. 1b).

The second step is to subdivide the aerial strip to define zones that (1) account for more than 50% overlap between the aerial strip and the photo-ID distribution grid, and (2) contain more than 10 photo-ID reports per year$_2$ period to ensure sufficient sampling. Following these rules, 3 zones combining both information were defined: zones R, T, and W (see zones in Fig. 1b and associated characteristics in Table S1 in Supplement 2). Other zones, where photo-ID is not combined with aerial surveys, are defined based on variations in the geomorphology of the reef and coastline or following administrative boundaries where no geomorphological changes are observed over large areas. Based on the small home range fidelity of green and hawkbill turtles in neritic habitats, we assumed that the chosen subdivision of the study area allowed sampling of independent populations.

In total, the aerial strip was divided into 25 zones (average area = 2.4 ± 1.2 km^2). For each zone, the average depth and bathymetric slope were calculated from the isobaths retrieved from HYDRORUN (Ropert & Lazure 2011) (see Table S1 for details).

2.2.2. Density estimated from the aerial survey

The pilot was provided only with the start and end points and the approximate strip width, resulting in variable transect lengths (L) across flights (L_{North} =

50 ± 9 km; L_{South} = 35 ± 5 km). To account for this variability, we used linear encountered density (LED), defined as the count divided by transect length (turtles km^{-1}), rather than direct counts as an abundance index. Distance sampling (Buckland et al. 2005), commonly used in aerial surveys (Benson et al. 2007, 2020, Lauriano et al. 2014), was not applicable here due to the sinusoidal trajectory and difficulty estimating perpendicular distances without physical markers on the aircraft, which was flown with open doors. We also assume that availability bias (the presence of animals at the surface) is uniformly distributed and constant over time (Benson et al. 2007, 2020, Lauriano et al. 2011, Fuentes et al. 2015), and since we aim to measure trends in abundance using a consistent index, this bias is not included.

Several environmental factors may influence sea turtle counts: (1) solar glare, represented by hours after sunrise ('sunhours'); (2) seasonality, affecting turtle surface availability and coastal presence ('months'); and (3) weather conditions, which may differ from forecasts despite pre-flight selection, potentially impacting detection efficiency ('conditions'). Additionally, inter-observer bias may arise from multiple observers conducting surveys over 16 yr. To account for these factors, we evaluated several linear models, including mixed-effects models (*mixedlm* and *ols* from the *statsmodels* v.0.14.1 Python library), to predict LED regionally (north and south) and zonally (25 zones) over time ('$year_2$'). Model selection was performed in 2 stages. Firstly, models incorporating combinations of environmental parameters ('sunhours', 'months', 'conditions') were compared using the Akaike information criterion (AIC) to identify significant predictors. Secondly, we evaluated whether including 'observer' as a random effect improved model fit by assessing explained variance and comparing AIC values.

To meet statistical assumptions, LED values were log-transformed for normality, confirmed with the Shapiro-Wilk test, and homoscedasticity was verified using Levene's test. Linear regressions of regional and zonal LED time series were then used to estimate trend slopes and residual standard deviations, providing insights into temporal and spatial variability.

2.2.3. Size class estimated from the aerial survey

The reported size class covariate is highly dependent on both elevation and observer. Elevation varies mostly from flight to flight (SD = 40 m) and only slightly within a flight (F-statistic = 398, $p < 0.05$). The observer, who has no clear visual size reference in the ocean, also classifies individuals relatively from one to another. We therefore regrouped the categories 'small' and 'medium' into a larger category called 'small' (N_{small}), which was more likely to represent juveniles (straight carapace length [SCL] < 1 m) to be compared to 'large' individuals (N_{large}) which was more likely to represent adults (SCL > 1 m). The ratio between these 2 categories, hereinafter referred to as R_s, was predicted using a mixed linear model with 'elevation' and '$year_2$' as fixed effects and 'observer' as a random effect (see Eq. 1). A prediction was made for each region (north and south), checking that the assumptions of residual normality and homoscedasticity were valid:

$$R_s = \frac{N_{small}}{N_{small} + N_{large}} \sim year_2 + elevation + \left(1 \mid observer\right) \quad (1)$$

R_s was predicted for an elevation of 200 m corresponding to the average altitude above the water surface.

2.2.4. Species, life stage, and site fidelity estimated from photo-ID

Regional (north/south) or zonal statistics were calculated using all distinguishable individuals. The maximum number of identifiable individuals included those with both profiles recorded, along with those reported only with the right profile. Individuals reported only with the left profile were excluded, as it cannot be determined whether isolated left and right profiles belong to the same animal. Identified individuals were classified into 4 categories: 'Juvenile_Cm', 'Adult_Cm', 'Juvenile_Ei', and 'Adult_Ei', representing juvenile and adult green turtles and juvenile and adult hawksbill turtles, respectively. Juveniles were distinguished from adults using a combination of criteria, including visible sexual dimorphism, size estimation informed by environmental context, or prior knowledge of the individual (in the case of adults). If doubt remained, the life stage was recorded as 'NA'. Categorical proportions in zones R, T, and W, where aerial and photo-ID overlapped, were indexed to the LED variation estimated by the aerial survey for the corresponding years and zones. Overall statistics were evaluated based on all identified individuals throughout the study area. Site fidelity was estimated for all identified individuals reported at least 5 times over a minimum period of 2 yr. The approach was to measure, for each individual, the distance to the site where each individual was most frequently observed. Site fidelity was quantified by considering the 95% percentile interval of all distances to the primary observation site.

3. RESULTS

3.1. Survey summary

Between 2008 and 2023, a total of 154 aerial surveys were conducted, with 8 excluded due to GPS failure. Of the remaining surveys, 146 covered the north region, accumulating 80 h of flight time and a total distance of 7340 km, while 92 surveys covered the south region, accumulating 35 h and 3232 km. Across all surveys, observers recorded 8128 sea turtle sightings. Over the same area and period, 2248 green and hawksbill turtle sightings were reported through the photo-ID programme. This resulted in 418 positive identifications (with both profiles), 76 partial identifications with only the left profile, and 79 with only the right profile. Combining the confirmed identifications with single right-profile cases where the life stage was specified, the maximum number of distinct individuals identified was 497. Most of these individuals (472; 94%) were identified within the north region.

3.2. Abundance model selection

Using AIC, the most parsimonious model for predicting LED incorporates weather conditions as the sole influential environmental variable (Table 1, Eq. 2):

$$\log(\text{LED} + 1) \sim \text{Year}_2 + \text{Conditions} \quad (2)$$

This model demonstrated a significant positive effect of 'optimal' weather conditions on LED for both regions. Specifically, 'optimal' weather increased LED by 0.13 turtles km^{-1} ($p < 0.01$) in the north and 0.22 turtles km^{-1} ($p < 0.001$) in the south, compared to 'average' conditions. Other variables, such as 'months' and 'sunhours', did not improve model performance and were therefore excluded.

Including 'observer' as a random effect in the best-fitting linear model (Eq. 2) increased the AIC by more than 25 for both regions (Table 1) and contributed minimal (0.06 in the north) or no additional explained variance (in the south; see detailed results in Supplement 3). These results suggest that the inclusion of 'observer' does not improve model performance for predicting LED over time. LED predictions for all regions and zones were therefore made using the model depicted in Eq. (2) with 'conditions' set to 'optimal.' Following the guidelines of Harrison et al. (2018), all regional and zonal models were evaluated for the normality of residuals using the Shapiro-Wilk test ($p > 0.05$) and for homoscedasticity using the Breusch-Pagan test ($p > 0.05$).

Table 1. The 9 tested models and their ΔAIC values relative to the first model, based on n = 3 environmental variables fitted over the north and south regions. The first 7 models ($\log(\text{LED} + 1) \sim \text{Year}_2 + \text{env}_n$) are linear models created by combining the environmental variables to identify the most significant predictors. The eighth model ($\log(\text{LED} + 1) \sim \text{Year}_2 + \text{Condition} + (1 \mid \text{observer})$) incorporates a random effect into the best linear model to evaluate the impact of interobserver variability. LED: linear encountered density; year_2: 2 yr window. See Section 2.2.2 for definitions of the environmental variables

Environmental predictors (env_n)	n	Random effect	ΔAIC North	ΔAIC South
months + sunhours + conditions	3	X	0.00	0.00
months + sunhours	2	X	−0.07	4.89
months + conditions	2	X	−4.25	−2.21
sunhours + conditions	2	X	−8.56	−3.96
sunhours	1	X	−5.66	3.12
months	1	X	−4.17	5.86
conditions	1	X	−14.27	−8.52
X	0	X	−11.42	2.63
conditions	1	observer	28.11	25.92

3.3. Size-class model

For both size-class models (north and south), the assumptions of normality in residuals and homoscedasticity were met (see Supplement 4 for model fitting results). In both models, the variance attributed to the random effect ('observer') exceeded the residual variance, highlighting the critical role of accounting for interobserver variability in size-class ratio (R_s) estimations. Moreover, excluding the random effect ('observer') caused the residuals to violate the normality assumption. Therefore, interobserver variability was explicitly accounted for by including 'observer' as a random effect to estimate R_s (see Eq. 1). There was a small but statistically significant positive effect of 'elevation' on R_s for the southern model. Specifically, for each unit increase in altitude, R_s increases by 0.001, meaning that for every 100 m difference in altitude, the proportion of 'small' increases by 0.1 (10% more individuals classified as 'small'). This effect was not observed along the north region.

3.4. Trends in abundance

Sea turtle abundance increased over time in both the north and south regions, with regression slopes of 0.12 turtles

km^{-1} year$_2^{-1}$ (R^2 = 0.73) for the north, and 0.05 turtles km^{-1} year$_2^{-1}$ (R^2 = 0.43) for the south (Fig. 2a). The observed trends and variability in both regions were primarily driven by fluctuations in the abundance of 'small' individuals (Fig. 2b). The correlation between regional abundance and the abundance of 'small' individuals was very high (Pearson's r(north) = 0.99, Pearson's r(south) = 0.92, $p < 0.001$). In contrast, the abundance of 'large' individuals was more stable, with lower residual standard deviations (SD residuals(large; north) = 0.05 turtles km^{-1}; SD residuals(large; south) = 0.02 turtles km^{-1}), and showed modest positive trends in both regions (slope(large; north) = 0.03 turtles km^{-1} year$_2^{-1}$ and slope(large; south) = 0.03 turtles km^{-1} year$_2^{-1}$). During the common period (2012–2023), the percentage of 'small' turtles was similar in both regions: 76 ± (SD) 5.8% in the south and 75 ± 1.9% in the north.

Fig. 3a shows that the highest average abundance of sea turtles is concentrated in zones A–C and G–H in the south, and P–W in the north. Significant differences in average abundance were observed across different coastal geomorphologies (Kruskal-Wallis, H = 11.4, $p < 0.05$), with notably higher abundance in fringing reef zones. Spearman rank correlation analysis revealed a negative correlation between mean turtle abundance and both mean depth ($r_{Spearman}$ = −0.55, $p < 0.05$) and mean depth slope ($r_{Spearman}$ = −0.64, $p < 0.005$), indicating that turtles preferentially inhabit shallow, gently sloping areas. The upward trend in abundance was largely driven by the zones with the highest turtle concentrations (A–C, G–H, M, and P–W). Both variability and trends were localized to these zones, with no zone showing a negative trend over the study period (Fig. 3b). Additionally, a marginally significant trend toward higher density was observed in areas inside the marine reserve compared to those outside (U = 94, Mann-Whitney, p = 0.07). Two zones appear particularly dynamic: zone B in the south (SD residuals(B) = 0.64 turtles km^{-1}) and zone R in the north (SD residuals(R) = 0.53 turtles km^{-1}) (Fig. 3c).

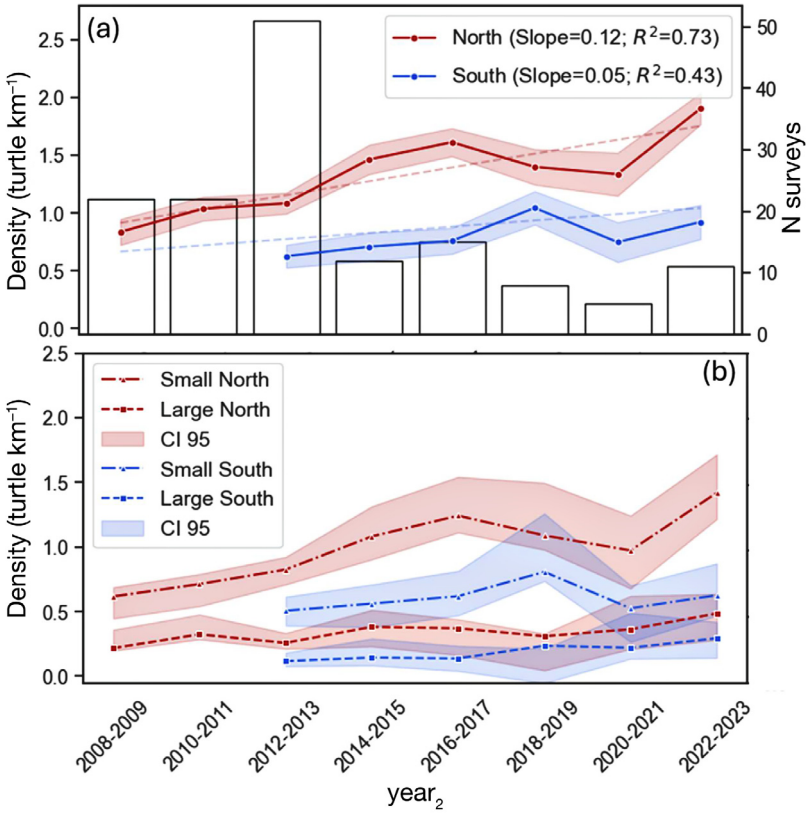

Fig. 2. (a) Regional trends in linear encountered density (LED) (red and blue dots; left axis) in the north (2008–2023) and south region (2012–2023), including 95% confidence intervals and linear regression lines with slopes and R^2 values (dotted lines). Aerial survey effort is shown as vertical bars (right axis), representing the number of surveys conducted within 2 yr intervals ('year$_2$'). (b) Regional trends in LED for 'small' and 'large' size classes across the north and south, with 95% confidence intervals

3.5. Trends in species and life stage

Based on the 497 individuals identified by photo-ID between 2008 and 2023, the west coast of Reunion Island shows an overall proportion of 77.8% juvenile green, 7.4% adult green, 14.4% juvenile hawksbill, and 0.4% adult hawksbill turtles. This proportion has varied over the years, with a minimum percentage of hawksbill turtles of 7.4% identified in 2010–2011 and a maximum of 26% in 2016–2017, all of which were juveniles.

Trends in species and life stage LED, estimated using a combination of aerial surveys and photo-ID data for zones R (Passe de l'Hermitage), T (St Gilles), and W (Cap La Houssaye), reveal that variations in abundance are primarily driven by fluctuations in the population of juvenile green turtles, which dominate all 3 zones (Fig. 4). The number of juvenile green turtles increased between 2008 and 2014, peaked between

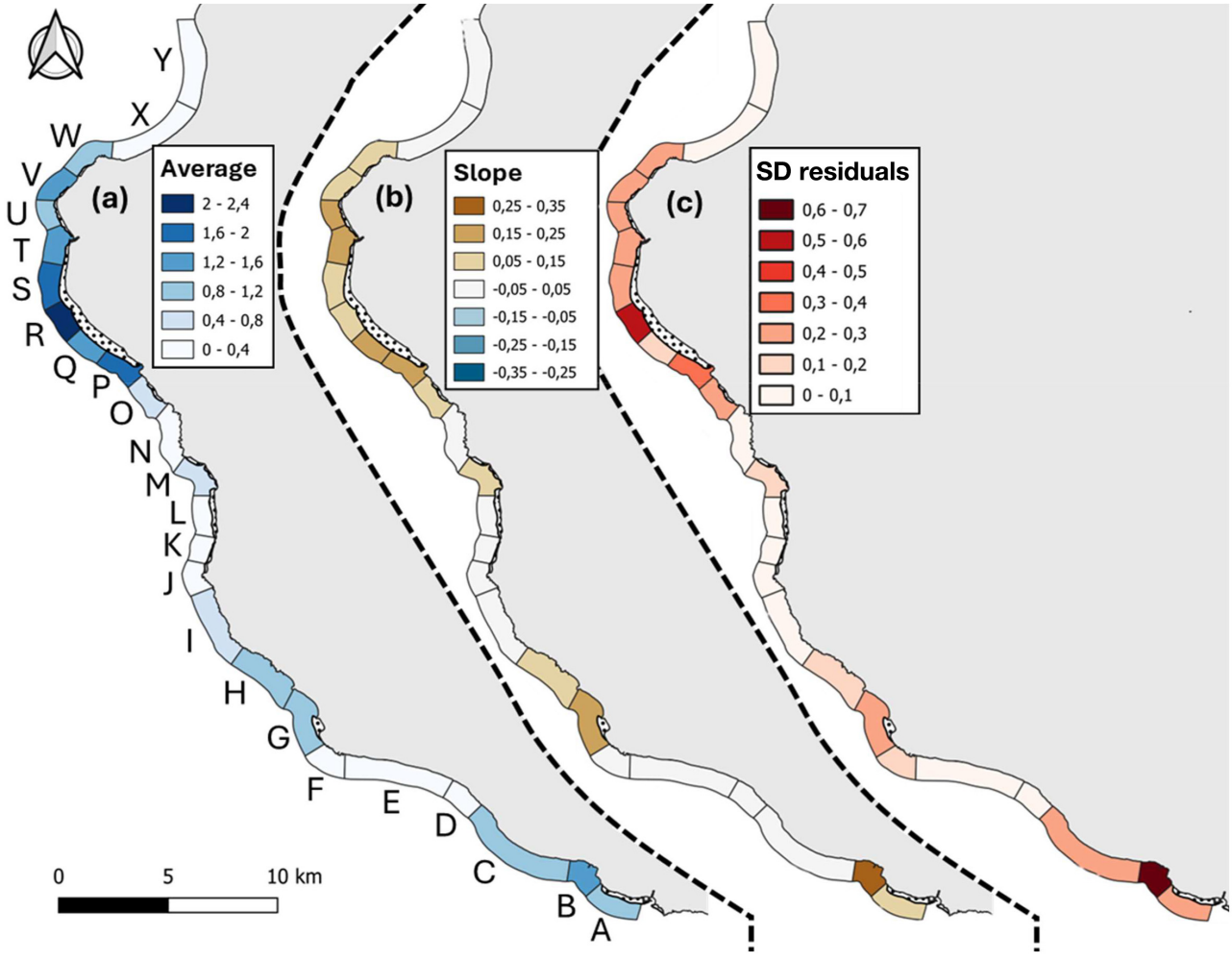

Fig. 3. (a) Zonal average linear encountered density (LED; turtles km^{-1}), (b) regression slope (turtles km^{-1} year$_2^{-1}$), and (c) standard deviation of residuals (turtles km^{-1}) for the time series of LED estimates obtained using the linear model. Spatiotemporal values of abundance are detailed in Supplement 5. year$_2$: 2 yr window

2014 and 2017, and then declined in all 3 zones. While in Cap La Houssaye (Zone W) and St Gilles (Zone T), the number of juvenile green turtles rebounded above its maximum level in 2022–2023, it remained low (~1.6 turtles km^{-1}) in Passe de l'Hermitage (Zone R). The highest level of adult green turtles is found at Passe de l'Hermitage (R), where the count has been stable at 0.2 turtles km^{-1} since 2008. At St Gilles (Zone T), the presence of adult green turtles increased from 0 in 2008–2009 to 0.5 turtles km^{-1} in 2022–2023 (+0.015 turtles km^{-1}; R^2 = 0.76). Only a limited number of adult green turtles (average = 0.02 ± 0.02 turtles km^{-1}) occupy Cap La Houssaye (W). Hawksbill turtles in the 3 zones is mainly represented by juveniles; only 1 adult was sighted in Cap La Houssaye (W) between 2012 and 2015. In Cap La Houssaye, the number of juveniles has been stable since 2008 (average = 0.11 ± 0.04 turtles km^{-1}). In St Gilles and Passe de l'Hermitage, the number of juvenile hawksbill turtles, which was absent in 2008, is slowly increasing (+0.007 turtles km^{-1}, R^2 = 0.76 in St Gilles; and +0.014 turtles km^{-1}, R^2 = 0.85 in Passe de l'Hermitage).

3.6. Site fidelity

Between 2008 and 2023, 105 individuals (86 juvenile greens, 7 adult greens, and 11 juvenile hawksbills) were sighted more than 5 times over at least 2 yr as part of the photo-ID programme. Of these, 64 individuals were monitored for at least 5 yr, 8 for 10 yr, and 2 adult greens for the entire study period (16 yr). Over the 105 individuals tracked during the 16 yr programme, the average time between the first and last

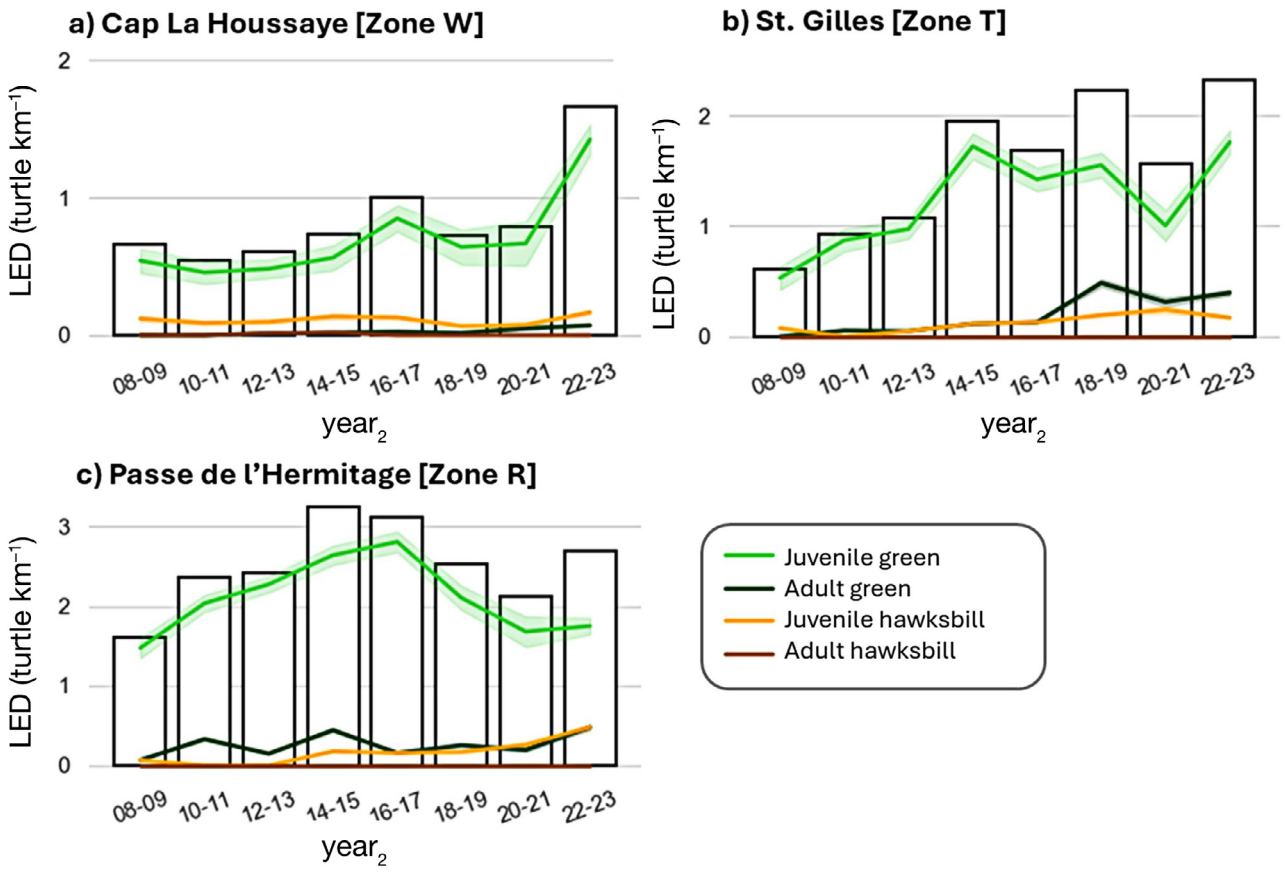

Fig. 4. Trends in life stage and species proportions derived from photo-ID data indexed on abundance trends (in linear encountered density, LED) estimated from aerial surveys in 3 zones: (a) W, (b) T, and (c) R. These zones represent areas where photo-ID data and aerial survey measurements overlap sufficiently and are considered valid for comparison (see Section 2.2.4). $year_2$: 2 yr window

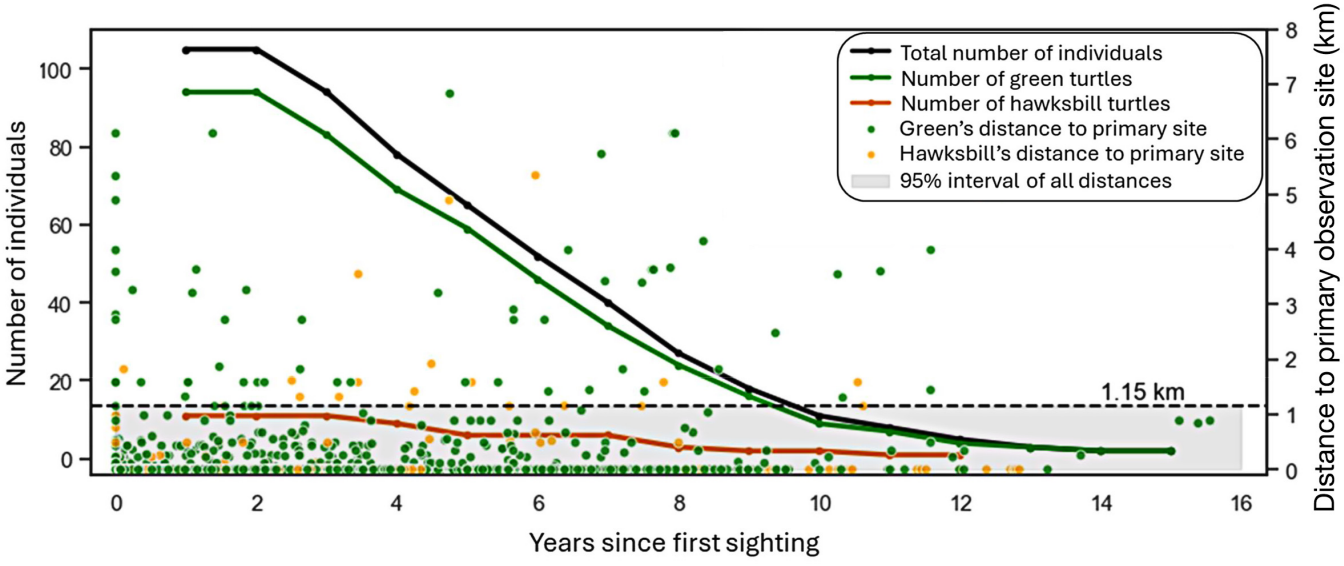

Fig. 5. Total number of individuals, green turtles, and hawksbill turtles sighted >5 times over at least 2 yr, along with their distances to the primary observation site. Each dot represents a report submitted through the photo-ID programme

sighting was 4.8 ± 2.2 yr for juvenile hawksbills, 5.9 ± 2.8 yr for juvenile greens, and 8.6 ± 1.6 yr for adult greens. The distribution of distances from each individual's primary observation site was highly skewed toward 0, with 78% of re-sightings occurring at the site where the individual was most frequently observed (Fig. 5). The 95th percentile of the distance distribution was 1.15 km from the primary observation site (1.11 km for green turtles and 1.58 km for hawksbill turtles).

4. DISCUSSION

This study offers a comprehensive overview of the trends in sea turtle distribution off the west coast of Reunion Island. Two survey methods were employed, both independently and in combination: aerial surveys, which deliver a broad perspective on spatiotemporal distribution (LED), and photo-ID, which provides detailed insights into population structure (life stage, species) and site fidelity.

4.1. Method strengths and limitations

The aerial survey designed in Reunion Island does not allow to provide an absolute estimate of abundance, as it is usually done over larger areas using distance sampling methods (Buckland et al. 2015). Instead, it aimed to provide an indication of trend and distribution through a consistent index. Unlike other studies using the 'zigzag' pattern, the area surveyed here is relatively small (60 km^2 versus more than 1000 km^2 in studies using zigzag pattern; Strindberg & Buckland 2004, Alves et al. 2013, 2016), which prevents us from following an invariant transect pattern here. Therefore, we adjust for inter-flight variability by using LED, which is the number of sighted turtles divided by the length of the transect, as an index of abundance. In addition, due to the difficulty in assessing the exact position of spotted turtles (wider unilateral field of view during curves vs. narrower bilateral field of view during straight legs), we evaluated LED by regions (north, south), and 25 zones.

To ensure the most reliable abundance index, we identified and addressed potential sources of bias. Observer efficiency bias is typically mitigated in aerial surveys using a double-count technique (Davis et al. 2022). However, in our case, the constraints of the microlight aircraft made it impossible to include an additional observer. Instead, observer variability was tested as a random effect in the model. As this did not improve model performance, it was excluded from the LED prediction. While this potential source of bias was challenging to evaluate, it appeared to have minimal influence on sea turtle counts. In contrast, observer variability significantly affected the estimation of size-class ratios and was therefore incorporated into the size-class ratio estimation model. Future advancements may enable the use of cameras or UAVs to standardize individual detections and size estimations independently of observers, as has been successfully demonstrated over a smaller area in the Chagos Archipelago (Stokes et al. 2023).

Other sources of potential environmental bias were evaluated, including sun glare, seasonality, and meteorological conditions. Sun glare did not appear to affect turtle counts, aligning with findings by Benson et al. (2007). This may be attributed to the fact that most surveys were conducted within a restricted time window shortly after sunrise (1–3 h). Seasonal temperature variations that influence sea turtle surface time (Lauriano et al. 2011, Roberts et al. 2022) could potentially induce higher detectability during winter months. However, no such pattern was observed in this study. This lack of variation may be due to the relatively small range of water temperatures in the coastal waters of Reunion Island (23–28°C; Conand et al. 2008), which likely does not induce significant variability in sea turtle surfacing behaviour. Regardless, seasonality does not impact the assessment of long-term trends in this study, as the analysis is based on 2 yr intervals. The final potential source of bias evaluated was meteorological conditions, which significantly influence sea turtle detectability by affecting sea surface roughness and, consequently, subsurface visibility (Luchinin 2016). Based on our findings, we strongly recommend incorporating meteorological conditions into abundance estimates in similar studies to enhance accuracy.

Due to the citizen science nature of the photo-ID programme, data are unevenly distributed in space and time, making it impossible to assess common population dynamics metrics such as recruitment, survival, population size, and others using capture–mark–recapture models (Kendall et al. 2019, Hudgins et al. 2023). However, while conclusions must be drawn with caution, the large number of observations collected over the 16 yr of the programme (n = 2248) provides considerable insight into turtle aggregation structures. Species and life stage proportions, although skewed towards a limited number of dive sites close to the coast and mainly in the north region, are well correlated with zones of high sea-turtle abundance from Trois-Bassins to Cap La Houssaye. This supports the

idea that these local observations cover a significant proportion of the northern aggregation and confirms the substantial contribution of this programme. Efforts should be made to advertise the photo-ID programme to other areas of high abundance that are currently poorly sampled, mostly in the south, in zones such as around Etang-Salé and St. Pierre.

Several studies have assessed sea turtle distribution and trends using aerial surveys (Roos et al. 2005, Lauriano et al. 2011, Fuentes et al. 2015, Benson et al. 2020, Pierantonio et al. 2023) or population structure from photo-ID programmes (Kendall et al. 2019, Hudgins et al. 2023). However, these 2 data sources have never been combined before. Given their fundamentally different nature, several precautions were necessary to ensure reliable integration. In this study, we applied 2 criteria: (1) at least 50% overlap in the spatial distributions of sampling effort over the entire study period, and (2) a minimum of 10 photo-ID reports per 2 yr period. It is worth noting that this relatively low threshold was met only twice in St. Gilles, while the average number of reports per 2 yr period was much higher: 69 in Passe de l'Hermitage, 44 in St. Gilles, and 132 in Cap La Houssaye. These strict criteria limited the combination of aerial and photo-ID data to 3 zones—the most abundant, the 7th most abundant, and the 13th most abundant—covering a total area of 5.5 km^2, or 9% of the surveyed area. Nevertheless, potential biases remain. Because photo-ID programmes are typically conducted near dive sites located along the coast or within the 10–30 m isobath zone, they are less likely to capture individuals occupying deeper habitats, which often include larger individuals (Blumenthal et al. 2009). This limitation can bias population estimates from photo-ID programmes toward juveniles. In addition, estimating size class from an elevation of approximately 200 m will result in a greater chance of missing small individuals relative to larger individuals, potentially skewing size-class estimates from aerial surveys toward larger individuals. These biases are consistent with the observed size-class proportions: 76% small to 24% large in aerial surveys, compared to 92% juveniles to 8% adults in photo-ID data. It is likely that the most realistic proportion of juveniles to adults lies somewhere in between these estimates.

4.2. Dynamics and structure of turtle distribution

This study demonstrates a slow but significant increase in sea turtle abundance along the west coast of Reunion Island between 2008 and 2023, with an estimated growth rate of 0.12 turtles km^{-1} $year_2^{-1}$ in the north region—equivalent to 1 additional turtle km^{-1} every 20 yr. Jean et al. (2010a) also observed an increase in abundance in the north region between 1998 and 2008. Although the protocols and abundance indices from these 2 periods are not directly comparable, their results collectively suggest that sea turtle abundance in the north region has steadily increased over the past 25 yr. Zones of high abundance are consistent between the 2 studies, with most turtles located between Trois-Bassins and Cap La Houssaye in the north. Our study revealed 2 additional hotspots in the south near Etang Salé and St. Pierre. Preliminary findings suggest that sea turtle densities may be increasing more rapidly within the marine reserve than outside it.

The inclusion of size class as a covariate in our analysis did not reveal spatial differences in turtle size between the north and south. Both aerial surveys and photo-ID data indicate that juvenile green and hawksbill turtles dominate the west coast of Reunion Island. This observation aligns with the findings of Chassagneux et al. (2013), who reported that 75% of green turtles and 78% of hawksbill turtles observed around Reunion Island were juveniles. These results reinforce the idea that Reunion Island primarily serves as a developmental habitat (Meylan et al. 2011).

Inter-annual variations in abundance appear to be driven primarily by changes in the number of juveniles, reflecting the transient nature of their presence in the neritic feeding grounds around Reunion Island. Juvenile turtles are typically resighted for shorter durations (5.0 ± 2.3 yr) than adults (8.6 ± 1.6 yr), despite exhibiting high site fidelity (95% observed within 1.1 km of their initial sighting). These findings suggest that juvenile turtles reside in these coastal waters for several years before relocating, likely transitioning through a sequence of developmental habitats before reaching maturity (Carr et al. 1978, Meylan et al. 2011). Several habitat shifts during the immature life stage have been documented through satellite tracking (Hart et al. 2012, Hays et al. 2021) and opportunistic recapture data (Whiting et al. 2010, von Brandis et al. 2017), further supporting this hypothesis.

The low proportion of adults as well as the slow increase in juveniles over time on the west coast of Reunion Island could be explained by the isolated location of Reunion Island in relation to the main nesting areas of hawksbill and green turtles in the southwest Indian Ocean (Mortimer et al. 2020, Van De Geer et al. 2022). Additionally, regional currents place Reunion Island at the periphery of neonate dispersal corridors (Jensen et al. 2020, Le Gouvello et al.

2024). The majority of observed adults are foraging individuals, as the island's nesting activity is limited (Ciccione & Bourjea 2006), thus reducing the proportion of adults compared to sites that support both nesting and foraging. In terms of species composition, the average green-to-hawksbill ratio over the 16 yr study period was approximately 85:15 along the west coast. This relatively low presence of hawksbill turtles can be attributed to 2 factors: (1) the smaller regional population of hawksbill turtles compared to green turtles, with green turtles producing approximately 10 times more egg clutches than hawksbills (Mortimer et al. 2020), and (2) the greater distance of major hawksbill nesting sites from Reunion Island compared to the closer proximity of green turtle nesting sites (Van De Geer et al. 2022).

The spatial distribution of sea turtles along the coast of Reunion Island shows that they favour fringing reef zones with shallow and low bathymetric slope. This could be related to the fact that green turtles, predominant in Reunion Island, have been shown to feed mainly on red algae (in particular *Carpopeltis* spp., *Amansia* spp., and *Ptilophora biserrata*), according to stomach content analyses (Ciccione 2001). Red algae are found at shallow depths of 10–30 m. This could explain why St. Leu, an important fringing reef zone with a steep bathymetric slope, has a low abundance of sea turtles compared to other fringing reef zones on the west coast. Another interesting result from the combination of aerial surveys and photo-ID is that the highest density of hawksbill turtles is found at Passe de l'Hermitage, which connects the outer reef slope to the largest reef flat of Reunion Island. In addition to shelter, the reef flat provides food resources that may explain some of the variability in abundance observed at Passe de l'Hermitage. The spatial extent of Corallimorphidae (*Rhodactis rhodostoma* and *Gyractis sesere*), on which hawksbills feed (León & Bjorndal 2002, Von Brandis et al. 2014), has increased significantly (Broudic et al. 2024), in line with the positive trend in the abundance of juvenile hawksbills. In parallel, the seagrass beds at l'Hermitage, which are uniquely composed of *Syringodium isoetifolium*, have a highly variable cover and have seen a steep decline since 2017, with a complete disappearance by 2020 (Ifrecor 2021). This food source for green turtles (Cuvillier et al. 2017, Mulochau et al. 2021) is consistent with the observed trends of juvenile green turtles, which increased until 2017 before sharply decreasing. Food type and availability and population structure seems then to be linked, confirming the potential of sea turtles as indicators of habitat health and attractiveness.

4.3. Conservation implications and future research

The increase in the number of in-water sea turtles on the west coast of Reunion Island between 2008 and 2023, and even since 1998, if we consider the results of Jean et al. (2010a) (in the north region), is a promising sign for sea turtle conservation. Locally, this positive trend can be attributed in part to the establishment of the Kelonia Care Centre, which has successfully treated 124 turtles since 2005, while also raising public awareness. Over the past decade (2013–2023), Kelonia has hosted more than 1.5 million visitors, further emphasizing its role in conservation efforts. Additionally, the creation of the Marine Protected Area in 2007 has contributed to the protection of the most important sea turtle habitats.

Regionally, the updated status of the green turtle from Vulnerable to Least Concern in the western Indian Ocean (Bourjea & Dalleau 2023) is consistent with the observed local trend on Reunion Island. For hawksbill turtles, the most recent regional assessment of conservation status (Hamann et al. 2022) observed positive signs of recovery in the Seychelles and Chagos Archipelagos, which account for 97% of the region's nesting hawksbill population (Mortimer et al. 2020, Van De Geer et al. 2022). This aligns with the trends observed in 2 of the 3 zones examined in this study. However, due to Reunion Island's isolation from major nesting sites, it remains unclear whether the observed increases are driven by regional population growth or the attractiveness of local habitats. It is likely that the trends on Reunion Island reflect the peripheral signal of a broader regional recovery. Similar connections have been established elsewhere, such as the strong link between foraging loggerhead turtle populations in the Azores and nesting trends in Florida (Vandeperre et al. 2019). While further investigation is needed, the steady recruitment of juveniles on Reunion Island is consistent with trends reported at most nesting sites across the region (Hamann et al. 2022).

Despite these encouraging signs, continued conservation efforts are essential, as anthropogenic threats remain significant and are increasing. Between 2000 and 2023, 72 boat strikes were recorded in Reunion Island's coastal waters, with a survival rate of only 10%. Alarmingly, the frequency of collisions has risen from an average of 2 per year (2000–2017) to 6 per year (2008–2023). Coral reef habitats, critical to sea turtles, have also suffered a 50% loss in coral cover over the past 40 yr due to water pollution and climate change (Broudic et al. 2024).

In this context, resuming and maintaining local aerial monitoring efforts is crucial for tracking long-term

trends in abundance and distribution of these vulnerable species. Moreover, our study demonstrates the significant contribution of citizen science photo-ID programmes on Reunion Island, which provide essential data to inform and support sea turtle conservation efforts.

Acknowledgements. This study was conducted as part of the HOME-RUN project, funded by DEAL-Réunion, France Nation Verte, Fonds Vert Réunion 2023, and CCT-Réunion 2019-2023. Aerial data were collected within the framework of the National Action Plan for marine turtles over French territories of the Indian Ocean, supported by DEAL-Réunion, Réunion des Musées Régionaux, Regional Council of Reunion Island, France Nation Verte, and Fonds Vert Réunion 2023, as well as the CHARC project, funded by EU-FEDER, DEAL-Réunion, and the Regional Council of Reunion Island. Photo-ID data were collected under the citizen science programme conducted by Kelonia and funded by Réunion des Musées Régionaux and the Regional Council of Reunion Island. We express our gratitude to the Reunion Natural Marine Reserve and DEAL-Réunion for permitting flights over the Marine Reserve. Special thanks to all observers who participated in the aerial survey programme and to all pilots from Felix ULM for their significant contributions to the success of the surveys, particularly Gérard Charles Bresse, Serge Farci, and Dorothée Blanc, for their patience and professionalism. We also thank all contributors to the photo-ID programme, and everyone involved in data management, including both interns and agents, especially Marie Lauret-Stepler for her role in the network animation. We acknowledge Sylvain Bonhommeau and Audrey Jaeger for their valuable counsel in statistical analysis. We sincerely thank Georges Hughes for his valuable contributions in correcting and improving the English language of the manuscript.

LITERATURE CITED

Aguirre AA, Lutz PL (2004) Marine turtles as sentinels of ecosystem health: Is fibropapillomatosis an indicator? EcoHealth 1:275–283

Aguirre AA, O'Hara TM, Spraker TR, Jessup DA (2002) Monitoring the health and conservation of marine mammals, sea turtles, and their ecosystems. Oxford University Press, New York, NY

Alves MD, Schwamborn R, Borges JCG, Marmontel M, Costa AF, Schettini CAF, de Araújo ME (2013) Aerial survey of manatees, dolphins and sea turtles off northeastern Brazil: correlations with coastal features and human activities. Biol Conserv 161:91–100

Alves MD, Kinas PG, Marmontel M, Borges JCG, Costa AF, Schiel N, Araújo ME (2016) First abundance estimate of the Antillean manatee (*Trichechus manatus manatus*) in Brazil by aerial survey. J Mar Biol Assoc UK 96:955–966

Ballorain K, Ciccione S, Bourjea J, Grizel H, Enstipp M, Georges JY (2010) Habitat use of a multispecific seagrass meadow by green turtles *Chelonia mydas* at Mayotte Island. Mar Biol 157:2581–2590

Benson SR, Forney KA, Harvey JT, Carretta JV, Dutton PH (2007) Abundance, distribution, and habitat of leatherback turtles (*Dermochelys coriacea*) off California, 1990–2003. Fish Bull 105:337–347

Benson SR, Forney KA, Moore JE, LaCasella EL, Harvey JT, Carretta JV (2020) A long-term decline in the abundance of endangered leatherback turtles, *Dermochelys coriacea*, at a foraging ground in the California Current Ecosystem. Glob Ecol Conserv 24:e01371

Bertrand J, Bonnet B, Lebrun G (1986) Nesting attempts of *Chelonia mydas* at Reunion Island (SW Indian Ocean). Mar Turtle Newsl 39:3–4

Berube MD, Dunbar SG, Rützler K, Hayes WK (2012) Home range and foraging ecology of juvenile hawksbill sea turtles (*Eretmochelys imbricata*) on inshore reefs of Honduras. Chelonian Conserv Biol 11:33–43

Blumenthal JM, Austin TJ, Bell CDL, Bothwell JB and others (2009) Ecology of hawksbill turtles, *Eretmochelys imbricata*, on a western Caribbean foraging ground. Chelonian Conserv Biol 8:1–10

Bourjea J, Dalleau M (2015) Oceanic connectivity by green turtle in the WIO. In: UNEP-Nairobi Conv WIOMSA 2015 Reg State Coast Rep West Indian Ocean UNEP WIOMSA Nairobi, p123–124

Bourjea J, Dalleau M (2023) *Chelonia mydas* (Southwest Indian Ocean subpopulation). The IUCN Red List of Threatened Species 2023: e.T220970396A220970430. https://dx.doi.org/10.2305/IUCN.UK.2023-1.RLTS.T220970396A220970430.en

Broudic L, Pinault M, Romain C (2024) Etat écologique des récifs coralliens de La Réunion 2021-2023-Rapport d'activité 3-UTOPIAN. BESTRUN

Buckland ST, Anderson DR, Burnham KP, Laake JL (2005) Distance sampling. In: Armitage P, Colton T (eds) Encyclopedia of biostatistics, 1st edn. Wiley, Chichester

Buckland ST, Rexstad EA, Marques TA, Oedekoven CS (2015) Distance sampling: methods and applications. Springer, New York, NY

Carr AF, Carr MH, Meylan AB (1978) The ecology and migrations of sea turtles. 7, The West Caribbean green turtle colony. Bull Am Mus Nat Hist 162:1

Caughley G (1977) Sampling in aerial survey. J Wildl Manag 41:605–615

Chambault P, Dalleau M, Nicet JB, Mouquet P and others (2020) Contrasted habitats and individual plasticity drive the fine scale movements of juvenile green turtles in coastal ecosystems. Mov Ecol 8:1

Chassagneux A, Jean C, Bourjea J, Ciccione S (2013) Unraveling behavioral patterns of foraging hawksbill and green turtles using photo-identification. Mar Turtle Newsl 137: 1–5

Ciccione S (2001) Autopsie de tortues marines *Chelonia mydas*, retrouvées mortes à la Réunion. Bull Phaethon 13: 14–15

Ciccione S, Bourjea J (2006) Nesting of green turtles in Saint Leu, Réunion Island. Mar Turtle Newsl 112:1–3

Conand F, Marsac F, Tessier E, Conand C (2008) A ten-year period of daily sea surface temperature at a coastal station in Reunion Island, Indian Ocean (July 1993–April 2004): patterns of variability and biological responses. West Indian Ocean J Mar Sci 6:1–16

Cuvillier A, Villeneuve N, Cordier E, Kolasinski J, Maurel L, Farnier N, Frouin P (2017) Causes of seasonal and decadal variability in a tropical seagrass seascape (Reunion Island, south western Indian Ocean). Estuar Coast Shelf Sci 184:90–101

Davis KL, Silverman ED, Sussman AL, Wilson RR, Zipkin EF (2022) Errors in aerial survey count data: identifying pitfalls and solutions. Ecol Evol 12:e8733

Deschamps H (1962) Albert Lougnon : sous le signe de la tortue (voyages anciens à l'Ile 1611–1725). Outre-Mers Rev Hist 49:281

Dunbar SG, Anger EC, Parham JR, Kingen C and others (2021) HotSpotter: using a computer-driven photo-ID application to identify sea turtles. J Exp Mar Biol Ecol 535:151490

Frazier J (1975) Marine turtles of the western Indian Ocean. Oryx 13:164–175

Fuentes MMPB, Lawler IR, Gyuris E (2006) Dietary preferences of juvenile green turtles (*Chelonia mydas*) on a tropical reef flat Mariana. Channels 33:671–678

Fuentes MMPB, Bell I, Hagihara R, Hamann M and others (2015) Improving in-water estimates of marine turtle abundance by adjusting aerial survey counts for perception and availability biases. J Exp Mar Biol Ecol 471:77–83

Halpern BS, Walbridge S, Selkoe KA, Kappel CV and others (2008) A global map of human impact on marine ecosystems. Science 319:948–952

Hamann M, Godfrey MH, Seminoff JA, Arthur K and others (2010) Global research priorities for sea turtles: informing management and conservation in the 21st century. Endang Species Res 11:245–269

Hamann M, Flavell F, Frazier J, Limpus CJ, Miller JD, Mortimer JA (2022) Assessment of the conservation status of the hawksbill turtle in the Indian Ocean and South-East Asia region. https://www.cms.int/iosea-turtles/sites/default/files/publication/iosea_hawksbill_assessment_2022.pdf

Harrison XA, Donaldson L, Correa-Cano ME, Evans J and others (2018) A brief introduction to mixed effects modelling and multi-model inference in ecology. PeerJ 6:e4794

Hart KM, Sartain AR, Fujisaki I, Pratt HL, Morley D, Feeley MW (2012) Home range, habitat use, and migrations of hawksbill turtles tracked from Dry Tortugas National Park, Florida, USA. Mar Ecol Prog Ser 457:193–207

Hays GC, Mortimer JA, Rattray A, Shimada T, Esteban N (2021) High accuracy tracking reveals how small conservation areas can protect marine megafauna. Ecol Appl 31:e02418

Hudgins JA, Hudgins EJ, Köhnk S, Mohamed Riyad E, Stelfox MR (2023) A brighter future? Stable and growing sea turtle populations in the Republic of Maldives. PLOS ONE 18:e0283973

Hughes GR (1974) The sea turtles of South East Africa. The Oceanographic Research Institute, Durban

Ifrecor (2021) Etat de santé des récifs coralliens, herbiers marins et mangroves des outre-mer français. Bilan 2020. https://ifrecor.fr/bilan-etat-de-sante-2020/

INSEE (2025) Populations légales 2021 — 974 La Réunion. Institut national de la statistique et des études économiques. https://www.insee.fr/fr/statistiques/2011101?geo=DEP-974#consulter-sommaire

Jean C, Ciccione S, Ballorain K, Georges JY, Bourjea J (2010a) Ultralight aircraft surveys reveal marine turtle population increases along the west coast of Reunion Island. Oryx 44:223–229

Jean C, Ciccione S, Talma E, Ballorain K, Bourjea J (2010b) Photo-identification method for green and hawksbill turtles—first results from Reunion. Indian Ocean Turtle Newsl 11:8–13

Jensen MP, Dalleau M, Gaspar P, Lalire M and others (2020) Seascape genetics and the spatial ecology of juvenile green turtles. Genes (Basel) 11:278

Kendall WL, Stapleton S, White GC, Richardson JI, Pearson KN, Mason P (2019) A multistate open robust design: population dynamics, reproductive effort, and phenology of sea turtles from tagging data. Ecol Monogr 89:e01329

Komoroske LM, Lewison RL, Seminoff JA, Deheyn DD, Dutton PH (2011) Pollutants and the health of green sea turtles resident to an urbanized estuary in San Diego, CA. Chemosphere 84:544–552

Lauriano G, Panigada S, Casale P, Pierantonio N, Donovan GP (2011) Aerial survey abundance estimates of the loggerhead sea turtle *Caretta caretta* in the Pelagos Sanctuary, northwestern Mediterranean Sea. Mar Ecol Prog Ser 437:291–302

Lauriano G, Pierantonio N, Donovan G, Panigada S (2014) Abundance and distribution of *Tursiops truncatus* in the Western Mediterranean Sea: an assessment towards the Marine Strategy Framework Directive requirements. Mar Environ Res 100:86–93

Le Gouvello DZM, Heye S, Harris LR, Temple-Boyer J and others (2024) Dispersal corridors of neonate sea turtles from dominant rookeries in the Western Indian Ocean. Ecol Modell 487:110542

León YM, Bjorndal KA (2002) Selective feeding in the hawksbill turtle, an important predator in coral reef ecosystems. Mar Ecol Prog Ser 245:249–258

Luchinin AG (2016) Ocean optics — air and sea interface. In: Encyclopedia of optical engineering. CRC Press, Boca Raton, FL, p 1534–1542

Lutcavage ME, Plotkin PT, Witherington B, Lutz PL (1997) Human impacts on sea turtle survival. In: Lutz P, Musick J (eds) The biology of sea turtles. CRC Press, Boca Raton, FL, p 387–410

Makowski C, Seminoff JA, Salmon M (2006) Home range and habitat use of juvenile Atlantic green turtles (*Chelonia mydas* L.) on shallow reef habitats in Palm Beach, Florida, USA. Mar Biol 148:1167–1179

Meylan PA, Meylan AB, Gray JA (2011) The ecology and migrations of sea turtles 8. Tests of the developmental habitat hypothesis. Bull Am Mus Nat Hist 2011:1–70

Mortimer JA, Donnelly M (2008) *Eretmochelys imbricata*. The IUCN Red List of Threatened Species 2008: e.T8005A12881238. https://dx.doi.org/10.2305/IUCN.UK.2008.RLTS.T8005A12881238.en

Mortimer JA, Esteban N, Guzman AN, Hays GC (2020) Estimates of marine turtle nesting populations in the southwest Indian Ocean indicate the importance of the Chagos Archipelago. Oryx 54:332–343

Mulochau T, Jean C, Gogendeau P, Ciccione S (2021) Green sea turtle, *Chelonia mydas*, feeding on *Synapta maculata* (Holothuroidea: Synaptidae) on a seagrass bed (*Syringodium isoetifolium*) at Reunion Island, western Indian Ocean. Bêche-de-Mer Inf Bull 41:37–39

Nivière M, Dalleau M, Bourjea J, Jean C and others (2024) Intra-species variability in migratory movement of hawksbill turtles in the southwest Indian Ocean. Endang Species Res 53:379–393

Philippe JS, Bourjea J, Ciccione S (2016) Plan national d'actions en faveur des tortues marines sur les territoires français du sud-ouest de l'océan Indien 2015–2020. La Réunion. Volume 3. https://archimer.ifremer.fr/doc/00347/45777/45422.pdf

Pierantonio N, Panigada S, Lauriano G (2023) Quantifying abundance and mapping distribution of loggerhead turtles in the Mediterranean Sea using aerial surveys: implications for conservation. Diversity (Basel) 15:1159

Reisser J, Proietti M, Kinas P, Sazima I (2008) Photographic identification of sea turtles: method description and val-

idation, with an estimation of tag loss. Endang Species Res 5:73–82
Roberts KE, Garrison LP, Ortega-Ortiz J, Hu C and others (2022) The influence of satellite-derived environmental and oceanographic parameters on marine turtle time at surface in the Gulf of Mexico. Remote Sens 14:4534
Roos D, Pelletier D, Ciccione S, Taquet M, Hughes G (2005) Aerial and snorkelling census techniques for estimating green turtle abundance on foraging areas: a pilot study in Mayotte Island (Indian Ocean). Aquat Living Resour 18: 193–198
Ropert M, Lazure P (2011) Projet HYDRORUN: Etat d'avancement du projet Ifremer-OIHYDRORUN. Première année (2010). https://archimer.ifremer.fr/doc/00039/14992/
Sanchez CL, Bunbury N, Mortimer JA, A'Bear L and others (2024) Small-scale movements and site fidelity of two sympatric sea turtle species at a remote atoll. Mar Biol 171:91
Sauvignet H, Pavitrin A, Ciccione S, Roos D (2000) Premiers résultats des campagnes de dénombrements aériens des tortues marines sur la côte ouest de La Réunion. Bull Phaeton 11:8–12
Schofield G, Katselidis KA, Dimopoulos P, Pantis JD (2008) Investigating the viability of photo-identification as an objective tool to study endangered sea turtle populations. J Exp Mar Biol Ecol 360:103–108
Schofield G, Hobson VJ, Lilley MKS, Katselidis KA, Bishop CM, Brown P, Hays GC (2010) Inter-annual variability in the home range of breeding turtles: implications for current and future conservation management. Biol Conserv 143:722–730
Seminoff JA (2023) *Chelonia mydas*. The IUCN Red List of Threatened Species 2023: e.T4615A24765438. https://dx.doi.org/10.2305/IUCN.UK.2023-1.RLTS.T4615A247654386.en
Shimada T, Limpus CJ, Hamann M, Bell I, Esteban N, Groom R, Hays GC (2020) Fidelity to foraging sites after long migrations. J Anim Ecol 89:1008–1016
Siegwalt F, Benhamou S, Girondot M, Jeantet L and others (2020) High fidelity of sea turtles to their foraging grounds revealed by satellite tracking and capture-mark-recapture: new insights for the establishment of key marine conservation areas. Biol Conserv 250:108742
Stokes HJ, Mortimer JA, Laloë JO, Hays GC, Esteban N (2023) Synergistic use of UAV surveys, satellite tracking data, and mark-recapture to estimate abundance of elusive species. Ecosphere 14:e4444
Strindberg S, Buckland ST (2004) Zigzag survey designs in line transect sampling. J Agric Biol Environ Stat 9: 443–461
Turner J, Klaus R (2005) Coral reefs of the Mascarenes, Western Indian Ocean. Philos Trans R Soc A 363:229–250
Van De Geer CH, Bourjea J, Broderick AC, Dalleau M and others (2022) Marine turtles of the African east coast: current knowledge and priorities for conservation and research. Endang Species Res 47:297–331
Vandeperre F, Parra H, Pham CK, Machete M, Santos M, Bjorndal KA, Bolten AB (2019) Relative abundance of oceanic juvenile loggerhead sea turtles in relation to nest production at source rookeries: implications for recruitment dynamics. Sci Rep 9:13019
Von Brandis RG, Mortimer JA, Reilly BK, Van Soest RWM, Branch GM (2014) Diet composition of hawksbill turtles (*Eretmochelys imbricata*) in the Republic of Seychelles. West Indian Ocean J Mar Sci 13:81–91
Von Brandis RG, Mortimer JA, Van De Geer C, Lea JS (2017) A long migratory record for a small post-pelagic hawksbill. Mar Turtle Newsl 152:13–15
Wallace BP, Bandimere AN, Abreu-Grobois FA, Acosta H and others (2025) Updated global conservation status and priorities for marine turtles. Endang Species Res 56:247–276
Whiting SD, Macrae I, Murray W, Thorn R, Flores T, Joynson-Hicks C, Hashim S (2010) Indian Ocean crossing by a juvenile hawksbill turtle. Mar Turtle Newsl 129:16–17

Editorial responsibility: Sandra Hochscheid, Napoli, Italy
Reviewed by: J.A. Mortimer, S.E. Piacenza and 1 anonymous referee
Submitted: July 22, 2024; Accepted: February 11, 2025
Proofs received from author(s): April 22, 2025